



LAWRENCE  
LIVERMORE  
NATIONAL  
LABORATORY

# Numerical Modeling of Neoclassical Transport and Geodesic Acoustic Mode (GAM) Relaxation in a Tokamak Edge

M. Dorf, R. H. Cohen , J. C. Compton, M. Dorr, J.  
Hittinger, T. D. Rognlien, P. Colella, D. Martin, P.  
McCorquodale

September 19, 2012

The 24th IAEA Fusion Energy Conference  
San Diego, CA, United States  
October 8, 2012 through October 13, 2012

## **Disclaimer**

---

This document was prepared as an account of work sponsored by an agency of the United States government. Neither the United States government nor Lawrence Livermore National Security, LLC, nor any of their employees makes any warranty, expressed or implied, or assumes any legal liability or responsibility for the accuracy, completeness, or usefulness of any information, apparatus, product, or process disclosed, or represents that its use would not infringe privately owned rights. Reference herein to any specific commercial product, process, or service by trade name, trademark, manufacturer, or otherwise does not necessarily constitute or imply its endorsement, recommendation, or favoring by the United States government or Lawrence Livermore National Security, LLC. The views and opinions of authors expressed herein do not necessarily state or reflect those of the United States government or Lawrence Livermore National Security, LLC, and shall not be used for advertising or product endorsement purposes.

# Numerical Modeling of Neoclassical Transport and Geodesic Acoustic Mode (GAM) Relaxation in a Tokamak Edge

M. A. Dorf<sup>1</sup>, R. H. Cohen<sup>1</sup>, J. C. Compton<sup>1</sup>, M. Dorr<sup>1</sup>, J. Hittinger<sup>1</sup>, T. D. Rognlien<sup>1</sup>, P. Colella<sup>2</sup>, D. Martin<sup>2</sup>, and P. McCorquodale<sup>2</sup>

<sup>1</sup>Lawrence Livermore National Laboratory, Livermore, CA 94550 USA

<sup>2</sup>Lawrence Berkeley National Laboratory, Berkeley CA 94720 USA

*E-mail contact of main author: dorf1@llnl.gov*

**Abstract.** The edge of a tokamak in a high confinement (H mode) regime is characterized by steep density gradients and a large radial electric field. Recent analytical studies demonstrated that the presence of a strong radial electric field consistent with a subsonic pedestal equilibrium modifies the conventional results of the neoclassical formalism developed for the core region. In the present work we make use of the recently developed gyrokinetic code COGENT to numerically investigate neoclassical transport in a tokamak edge including the effects of a strong radial electric field. The results of numerical simulations are found to be in good qualitative agreement with the theoretical predictions and the quantitative discrepancy is discussed. In addition, the present work investigates the effects of a strong radial electric field on the relaxation of geodesic acoustic modes (GAMs) in a tokamak edge. Numerical simulations demonstrate that the presence of a strong radial electric field characteristic of a tokamak pedestal can enhance the GAM decay rate, and heuristic arguments elucidating this finding are provided.

## 1. Introduction

The edge of a tokamak in a high-confinement (H mode) regime is characterized by steep density gradients and a large radial electric field. This strongly-sheared equilibrium electric field can significantly suppress turbulent transport [1], making an analysis of neoclassical transport in a tokamak pedestal of considerable importance. Recent analytical studies [2-3] demonstrated that the presence of a strong radial electric field of  $E_r \sim V_T B_\theta / c$ , which is consistent with a subsonic pedestal equilibrium, modifies the conventional results of the neoclassical formalism developed for the core region, where  $E_r \ll V_T B_\theta / c$  [4]. Here,  $V_T$  is the ion thermal velocity,  $B_\theta$  is the poloidal component of the magnetic field, and  $c$  is the speed of light. In particular, it has been shown that a strong radial electric field provides suppression of the neoclassical ion heat flux. In addition, it has been demonstrated for a weakly collisional (banana) regime that the poloidal ion flow can change its direction as compared with its core counterpart [2]. That finding was applied to elucidate the discrepancy between the conventional banana regime predictions and recent experimental measurements of impurity flow performed on Alcator C-Mod [5].

In the present work we make use of numerical simulations to investigate neoclassical transport in a tokamak edge, including the effects of a strong radial electric field. The results of the simulations are found to be in good qualitative agreement with the theoretical predictions in Ref. [2]. In particular, the change of the poloidal ion flow direction and the suppression of the ion heat flux are demonstrated. The quantitative discrepancy between the results of the

analytical theory and the numerical simulations is discussed. The simulations are performed with the 4D continuum gyro-kinetic code COGENT [6-8]. The code is distinguished by the use of a fourth-order finite-volume (conservative) discretization combined with arbitrary mapped multiblock grid technology (nearly field-aligned on blocks) to handle the complexity of divertor geometry with high accuracy. COGENT also includes a number of options for collision models. The present results have been obtained with the closed-flux-surface version of the code, and our future studies will extend the analysis to include the effects of ion orbit losses by making use of the newly available divertor version of the COGENT code, which includes both the pedestal and the scrape-off-layer (SOL) regions.

In addition, we investigate the effects of a strong radial electric field on the relaxation of geodesic acoustic modes (GAMs) in a tokamak edge. Geodesic acoustic modes [9] can play an important role in the L-H transition and in regulating turbulence, and it is therefore increasingly important to develop a detailed theoretical understanding of their relaxation process. In particular, it has been well understood that slow collisionless relaxation of long-wavelength GAMs, with  $k_{\perp}\rho_i \ll 1$ , occurs as the result of wave-particle interaction between GAMs and a small number of resonant particles from the high-energy tail of an ion distribution function [10]. Here,  $\rho_i$  denotes the ion gyroradius. In the present work, we provide simple heuristic arguments showing that a strong radial electric field, characteristic of a tokamak pedestal, can shift the resonant condition toward the bulk of the ion distribution, thereby increasing the number of resonant particles and enhancing the GAM decay rate. We find that the COGENT simulations support the heuristic predictions.

This paper is organized as follows: The simulation model is described in Sec. II. In Sec. III we summarize the results of neoclassical benchmark exercises and report on simulations with a strong radial electric field. Finally, in Sec. IV, we investigate the effects of a strong radial electric field on the relaxation of geodesic acoustic modes (GAMs).

## 2. COGENT simulation model

The present 4D version of the COGENT code (2 configuration space + 2 velocity space coordinates) solves axisymmetric electrostatic multi-species gyrokinetic Boltzman-Poisson equations for the gyrocenter distribution functions  $f_{\alpha}(\mathbf{R}, v_{\parallel}, \mu, t)$  and the electrostatic potential  $\Phi(\mathbf{R}, t)$ . Here,  $\mathbf{R}$  is the gyrocenter position coordinate,  $v_{\parallel}$  is the parallel velocity,  $\mu$  is the magnetic moment, and the corresponding kinetic equation is given by

$$\frac{\partial f_{\alpha}}{\partial t} + \frac{d\mathbf{R}_{\alpha}}{dt} \cdot \nabla f_{\alpha} + \frac{dv_{\parallel\alpha}}{dt} \frac{\partial f_{\alpha}}{\partial v_{\parallel}} = C_{\alpha}[f_{\alpha}], \quad (1)$$

where

$$d\mathbf{R}_{\alpha}/dt = \mathbf{V}_{\alpha,gc} = v_{\parallel} \mathbf{b} + \mathbf{V}_{\alpha,dr}, \quad (2)$$

$$dv_{\parallel\alpha}/dt = (-1/v_{\parallel\alpha} m_{\alpha}) \mathbf{V}_{\alpha,gc} \cdot (Z_{\alpha} \nabla \Phi + \mu \nabla B), \quad (3)$$

$\mathbf{V}_{\alpha,dr}$  is the magnetic drift velocity composed of the  $\mathbf{E} \times \mathbf{B}$  drift, curvature drift, and  $\nabla B$  drift [4],  $\mathbf{B} = B \mathbf{b}$  is the magnetic field with  $\mathbf{b}$  denoting the unit vector along the field, and  $C_{\alpha}[f_{\alpha}]$  is the collision operator. Several model collision operators have been implemented and tested in COGENT [6-7]. These include a model parallel drag-diffusion collision operator, the Lorentz operator, and the linearized Fokker-Plank collision operator in the form proposed by Abel et al. in Ref. [11].

The present version of the code utilizes a long wavelength approximation,  $k_{\perp}\rho_{\alpha} \ll 1$ , to represent the gyrokinetic Poisson equation for electrostatic potential variations in the form,

$$\Delta^2\Phi = 4\pi e \left( n_e - \sum_{\alpha} n_{\alpha,gc} \right) - 4\pi e^2 \sum_{\alpha} \frac{Z_{\alpha}^2}{m_{\alpha}\Omega_{\alpha}^2} \nabla_{\perp} \cdot (n_{\alpha,gc} \nabla_{\perp} \Phi). \quad (4)$$

Here,  $\rho_{\alpha} = V_{T,\alpha}/\Omega_{\alpha}$  is the particle thermal gyroradius,  $\Omega_{\alpha} = Z_{\alpha}eB/(m_{\alpha}c)$  is the cyclotron frequency,  $k_{\perp}^{-1}$  represents the characteristic length-scale for variations of the electrostatic potential,  $\nabla_{\perp} \equiv \nabla - \mathbf{b}(\mathbf{b} \cdot \nabla)$ , and  $n_{\alpha,gc}$  is the gyrocenter ion density. Electrons can be modelled either kinetically or through use of a Boltzmann (in the linear limit, adiabatic) approximation, with various options for the coefficient of the Boltzmann factor. In particular, for the single-ion-species simulations reported in this work we adopt the following model for the electron density

$$n_e = \langle n_{i0} \rangle \frac{\exp[e\Phi/T_e(\psi)]}{\langle \exp[e\Phi/T_e(\psi)] \rangle}. \quad (5)$$

Here,  $\psi$  is the poloidal flux function,  $\langle \rangle$  denotes a flux-surface average,  $T_e(\psi)$  corresponds to the electron temperature distribution across magnetic flux surfaces,  $n_{i0}(\mathbf{R})$  is the initial value of the gyrocenter ion density distribution, and  $Z_i=1$  is assumed.

It is important to remark that the axisymmetric gyrokinetic simulation model specified by Eqs. (1)-(4) is not accurate enough to adequately describe the slow evolution of a long wavelength ( $k_{\perp}L \sim 1$ ) neoclassical radial electric field in a quasi-stationary state [12], where the particle fluxes across the magnetic surfaces are, to order  $(\rho_i/L)^2$ , independent of the radial electric field (so-called intrinsic ambipolarity). Here,  $L$  is the characteristic length scale for the magnetic field variations. Therefore, we restrict our studies to the analysis of a not-intrinsically-ambipolar rapid initial relaxation of the local Maxwellian distribution toward a quasi-stationary state (neoclassical quasi-equilibrium) [13]. The subsequent slow evolution of the quasi-stationary state including the evolution of the ‘‘ambipolar’’ radial electric field that occurs along with the relaxation of the toroidal angular momentum on a time scale of order  $(\rho_i/L)^{-3}$  is not considered. Because the toroidal angular momentum remains nearly the same during the initial not-intrinsically-ambipolar rapid relaxation, the radial electric field corresponding to the relaxed quasi-stationary state is determined as a linear function of the initial toroidal angular momentum and the pressure gradient diamagnetic flows [13].

### 3. COGENT Simulations of Neoclassical Transport

We first briefly summarize the results of neoclassical benchmark simulations performed for the case of weak density and temperature gradients corresponding to the tokamak core region, i.e.,  $\kappa_n\rho_{i0} \ll 1$ ,  $\kappa_T\rho_{i0} \ll 1$  and  $E_r \ll V_TB_{\theta}/c$ . Here,  $\rho_{i0}$  is the poloidal ion gyroradius, and  $\kappa_n$  and  $\kappa_T$  are the characteristic radial gradients for variations of the ion density and temperature, respectively. Next, we present the results of neoclassical simulations corresponding to the H-mode pedestal case with  $\kappa_n\rho_{i0} \sim 1$  and  $E_r \sim V_TB_{\theta}/c$

#### 3.1. Neoclassical Benchmark Simulations in a Tokamak Core

The COGENT code has been verified in a variety of benchmark simulations including the self-consistent effects of the electrostatic potential variations. A detailed description of those studies can be found in Refs. [6-7]. Here, for illustrative purposes, we present the results of

the neoclassical simulations performed using the linearized Fokker-Plank collision operator in the form proposed by Abel et al. in Ref. [11]. The results of the neoclassical COGENT simulations shown in Fig. 1 are found to be in good agreement with the results of the NCLASS code [14] for the poloidal velocity coefficient,  $k = V_\theta Z_i e B / c T_i \kappa_T$ , and the Chang-Hinton predictions [15] for the ion heat diffusivity,  $k = Q / n_i T_i \kappa_T$ . Here,  $V_\theta$  is the ion poloidal velocity, and  $Q$  is the flux-surface-averaged radial ion heat flux.

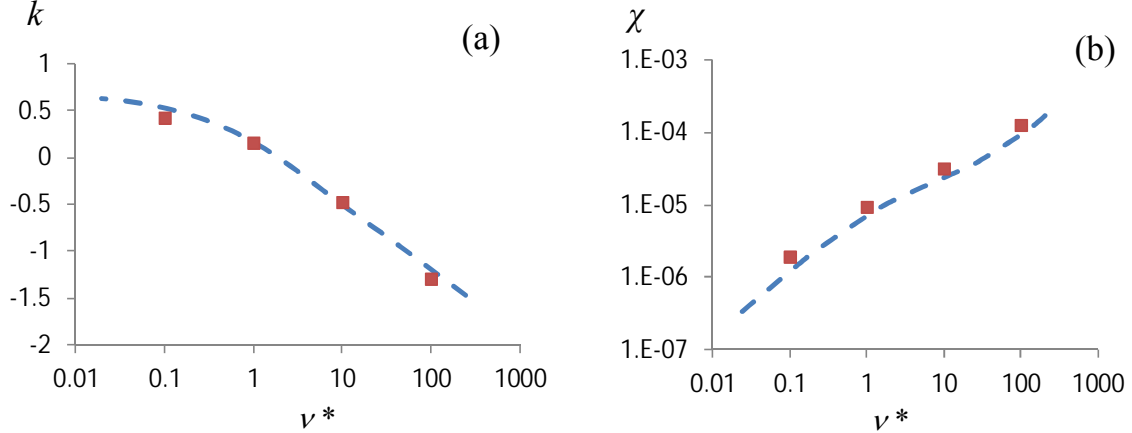


FIG 1. Plots of (a) the poloidal velocity coefficient,  $k$ , and (b) the ion heat diffusivity,  $\chi$ , versus the normalized collision frequency  $\nu^*$ . The results of the COGENT simulations (red dots) are compared with the results obtained with the NCLASS code [blue dashed curve in frame (a)], and the Chang-Hinton analytical approximation [blue dashed curve in frame (b)]. The parameters of the simulations correspond to  $\varepsilon=0.1$ ,  $q=1.2$ ,  $\rho_{i0}\kappa_n=\rho_{i0}\kappa_T=0.007$ ,  $\delta_i=1.7\times 10^{-5}$ . Here,  $\delta_i$  is the ratio of the ion gyroradius to the tokamak major radius, and  $\varepsilon$  and  $q$  are the inverse aspect ratio and magnetic safety factor, respectively. The results of the simulations are obtained for the case of a magnetic geometry with concentric circular flux surfaces. More details about these simulations can be found in Ref. [7].

### 3.2. Effects of a Strong Radial Electric Field

The properties of neoclassical transport can be significantly affected by the presence of a strong radial electric field corresponding to

$$E_r \sim V_T B_\theta / c. \quad (6)$$

A radial electric field of this magnitude can be present in the steep edge of a tokamak under H-mode conditions. Indeed, the length scale for plasma density variations in a tokamak edge can be of the order of the poloidal ion gyroradius,  $\kappa_n \rho_{i0} \sim 1$ , and the estimate for the electric field in Eq. (6) follows from the ion radial force balance, provided the ion toroidal flow velocity is less than the ion thermal velocity.

Recent analytical studies [2-3] showed that the presence of a strong radial electric field can modify the results of the conventional neoclassical formalism developed for the core region where  $E_r \ll V_T B_\theta / c$ . In particular, it was demonstrated for a weakly collisional (banana) regime that the poloidal ion flow can change its direction as compared with its core counterpart [2]. The modifications come primarily from the fact that the conventional neoclassical analysis neglects the  $E \times B$  drift velocity contribution to the poloidal advection term in the ion drift-kinetic equation. While this assumption is typically valid in the tokamak core region, the presence of a strong radial electric field in the edge [Eq. (6)] makes the contribution of the

$E \times B$  drift to the ion poloidal velocity comparable to the parallel streaming contribution, and therefore it can no longer be neglected [2-3]. Retaining the  $E \times B$  piece of the advection velocity in the analysis of the quasi-stationary neoclassical equilibrium has important consequences. In particular, the  $E \times B$  velocity modifies the shape of the boundary between trapped and passing particles, shifting it toward the tail of the ion distribution function. For a weakly collisional regime, this leads to a suppression of ion heat flux and a change in the poloidal flow direction [2].

Here, we make use of the closed-flux-surface version of the COGENT code to investigate the effects of a strong radial electric field [Eq. (6)] on the neoclassical transport properties in a weakly-collisional (banana) regime,  $v^* = 0.3$  [7]. The simulations include self-consistent variation of the electrostatic potential [Eqs. (4)-(5)] and adopt the linearized Fokker-Plank collision model [11]. Each data set, illustrated in Fig. 2, which plots the poloidal velocity coefficient and ion heat diffusivity versus normalized radial electric field, corresponds to an independent simulation distinguished by its value of the initial density gradient,  $\kappa_n$ . Note that while the density gradient is varied from  $\rho_{i\theta}\kappa_n \sim 0.1$  to  $\rho_{i\theta}\kappa_n \sim 2.0$ , the temperature gradient  $\rho_{i\theta}\kappa_T \sim 0.1$  is taken to be the same for all simulations and assumed to be shallow consistent with the analysis in Ref. [16].

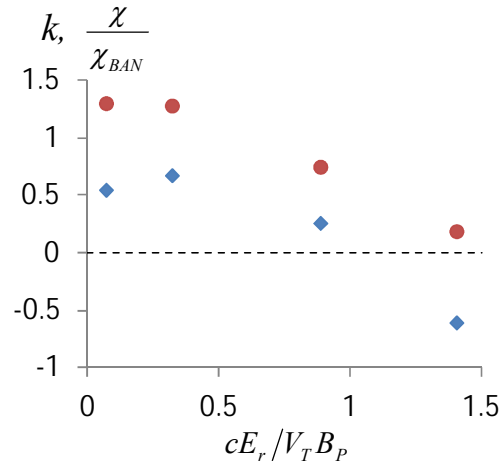


FIG 2. Plots of the poloidal velocity coefficient,  $k$  (blue diamonds), and the normalized ion heat diffusivity,  $\chi/\chi_{BAN}$  (red circles) evaluated at the inner midplane versus the normalized radial electric field. Here,  $\chi_{BAN}$  is the conventional neoclassical weakly-collisional ion heat diffusivity corresponding to the limit of  $v^* \ll 1$ ,  $\epsilon \ll 1$ , and  $cE_r/V_T B_p \ll 1$  (see, for instance, Ref. [4]). The parameters of the simulations are  $\epsilon = 0.03$ ,  $q = 1.2$ ,  $v^* = 0.3$ ,  $\rho_i/R_0 = 9.2 \times 10^{-5}$ . More details of the simulations can be found in Ref. [7].

Consistent with the analytical predictions in Ref. [2], the simulations recover a change in the poloidal velocity direction and a suppression of ion heat flux. However, there is also a pronounced quantitative discrepancy. The latter can plausibly be attributed to finite inverse aspect ratio ( $\epsilon$ ) corrections. Indeed, the analysis in Ref. [2] retains only the lowest order effects in  $\epsilon$ . For instance, in the limit of a small radial electric field  $E_r \ll V_T B_\theta/c$ , corresponding to the conventional neoclassical formalism, the analysis in Ref. [2] recovers  $k = 1.17$ . However, even for the case of  $\epsilon \approx 0.03$ , which is used in the present illustrative simulations, a more accurate estimate that takes into account finite  $\epsilon$  corrections, i.e.,  $k = 1.17(1 - 1.46 \times \epsilon^{1/2})$  [4] predicts a significantly different value,  $k = 0.88$ . Also, the differences between the linearized collision model used in COGENT and that used in Ref. [2] become increasingly important for finite values of  $\epsilon$ . Finally, for the case of steep density gradients,  $\kappa_n \rho_{i\theta} \sim 1$ , and a non-uniform

temperature distribution, nonlocal effects appear for finite values of  $\varepsilon$ . That is, variations in the ion density become pronounced on the banana-width length scale,  $\Delta_{ban} \sim \varepsilon^{1/2} \rho_{i0}$ . The analytical treatment in Ref. [2] assumes the local-theory limit ( $\kappa_n \Delta_{ban} \ll 1$ ), which implies  $\varepsilon^{1/2} \ll 1$ . However, this constraint is not well-satisfied in the present simulations corresponding to  $\varepsilon^{1/2} = 0.17$ . Also, note that the collisionality constraint for a weakly collisional (banana) regime, i.e.,  $\nu^* \ll 1$ , is not well-satisfied in the present simulations performed for  $\nu^* = 0.3$ . In principle, an attempt to reproduce the results of the analytical results quantitatively could be made by decreasing the collision frequency along with the inverse aspect ratio,  $\varepsilon$ . However, a significant decrease in the inverse aspect ratio below its present value of  $\varepsilon \approx 0.03$  would require simulation times beyond the scope of this initial study.

#### 4. Geodesic Acoustic Mode Relaxation in a Tokamak Edge

It has been well understood that slow collisionless relaxation of long-wavelength GAMs, with  $k_{\perp} \rho_i \ll 1$ , occurs as the result of wave-particle interaction between GAMs and passing particles, whose poloidal velocity satisfies the resonant condition,  $|\mathbf{v}_{\theta}^{res}|/a = \omega_{GAM}$  [10]. Here,  $\omega_{GAM} \sim V_T/R$  is the GAM frequency, and  $a$  and  $R$  are the tokamak minor and major radii, respectively. Assuming  $E_r \ll V_T B_{\theta}/c$ , which is typical for a tokamak core, it follows that  $\mathbf{v}_{\theta}^{res} \approx \mathbf{v}_{\parallel}^{res} B_{\theta}/B$ , and we readily obtain a well-known result,  $|\mathbf{v}_{\parallel}^{res}| \sim q V_T$ . Note that for the case of a large magnetic safety factor,  $q$ , ( $q \gg 1$ ), which is characteristic of the near-separatrix edge region, the number of resonant particles (and therefore the decay rate) becomes exponentially small.

The presence of a strong radial electric field  $E_r \sim V_T B_{\theta}/c$  in a tokamak pedestal can enhance the GAM decay rate. Indeed, the  $E \times B$  drift can now become comparable to the poloidal projection of a particle's parallel velocity, and the resonant condition reads

$$|\mathbf{v}_{\parallel}^{res} B_p/B + c E_r/B| \sim V_T a/R. \quad (7)$$

This condition has two solutions for the resonant parallel velocity, which are shifted from  $\pm q V_T$  values due to the presence of the  $E \times B$  drift. One solution is shifted downward the bulk of the particle distribution function and the other toward its tail. It is, however, straightforward to show (for a large safety factor,  $q$ ) that the net shift in the resonant velocities provides an increase in the number of the resonant particles, and therefore the GAM decay rate increases.

In order to test these heuristic predications we have performed model simulations of the collisionless GAM decay by making use of the closed-flux-surface version of the COGENT code. Previously, the code was successfully verified in benchmark simulations of the collisionless GAM relaxation for the case where the GAM perturbations are excited about a uniform density and temperature plasma equilibrium [8]. Here, we perform simulations of the collisionless GAM decay for the case where the GAMs are excited about a steep density gradient equilibrium,  $\kappa_n \rho_{i0} \sim 1$ . The temperature profile is taken to be uniform.

For these simulations we consider an annular geometry,  $r_{min} < r < r_{max}$ , with doubly periodic boundary conditions and radially-constant metric coefficients. The ion distribution function is initialized as a non-rotating local Maxwellian distribution with a periodic density profile,  $n = n_0 \{1 + \Delta_n \cos[2\pi(r-r_0)/\Delta_r]\}$ , where  $r_0 = (r_{max} + r_{min})/2$ , and  $\Delta_r = r_{max} - r_{min}$ . We make use of a particle- and momentum-conserving Krook model [6-7] to simulate the initial relaxation toward a neoclassical steady state, where the radial electric field builds up to balance the

pressure gradient. Once the neoclassical steady state is reached, the collisions are turned off adiabatically, and then a small sinusoidal perturbation in the ion density,  $n_1 = \delta_n \sin[2\pi(r-r_0)/\Delta_r]$ , is introduced to excite the GAM perturbations. The results of the numerical simulations corresponding to a uniform density equilibrium ( $\Delta_n=0$ ), and a steep density gradient equilibrium ( $\Delta_n=0.5$ ) are shown in Figs. 3(a). It is readily seen that the presence of a strong radial electric field  $|E_{r,max}| \approx 0.85 \times V_T B_\theta / c$  (corresponds to  $\Delta_n=0.5$ ) enhances the GAM decay rate consistent with the heuristic predictions. Here,  $|E_{r,max}|$  corresponds to the maximum value of the self-consistent equilibrium radial electric field.

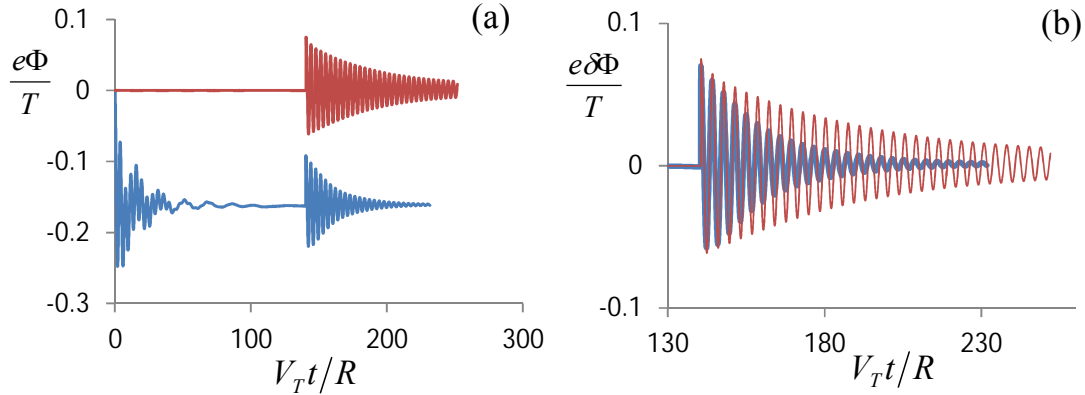


FIG 3. Collisionless GAM relaxation. (a) The evolution of the normalized electrostatic potential  $e\Phi/T$  for the cases of a uniform density equilibrium with  $\Delta_n=0$ ,  $E_r=0$  (red curve) and a steep density gradient equilibrium with  $\Delta_n=0.5$ ,  $|E_{r,max}| \approx 0.85 \times V_T B_\theta / c$  (blue curve). (b) The corresponding evolution of  $e\delta\Phi/T$ , where  $\delta\Phi(t) = \Phi(t) - \Phi_0$  is the potential perturbation about its neoclassical equilibrium value,  $\Phi_0$ . The parameters of the simulations are  $T=T_i=T_e$ ,  $2\pi\rho_s/\Delta_r=0.1$ ,  $\varepsilon=a/R=0.1$ , and  $q=3$ .

## 5. Conclusions

Here, we make use of the continuum gyro-kinetic code COGENT to investigate the influence of a strong radial electric field  $E_r \sim V_T B_\theta / c$  (characteristic of a tokamak pedestal under the H-mode conditions) on the properties of neoclassical transport and collisionless GAM relaxation. In particular, a change in the poloidal ion flow direction and a suppression of the ion heat flux are observed in a weakly-collisional regime and found to be in good qualitative agreement with the recent theoretical predictions in Ref. [2]. A quantitative discrepancy between the results of the analytical theory and the numerical simulations is discussed and shown likely due to a combination of finite aspect-ratio, finite orbit-size, and finite-collision-frequency effects. In addition, it is demonstrated that the presence of a strong radial electric field can enhance the GAM decay rate. While the present simulations are performed with the closed-flux-surface version of the code, our future work will extend the analysis to include the effects of ion orbit losses by making use of the newly available divertor version of the COGENT code, which includes both the pedestal and the scrape-off-layer regions.

## Acknowledgments

Work performed for the US Department of Energy under the auspices of the Lawrence Livermore National Laboratory under Contract DE-AC52-07NA27344 and of the Lawrence

Berkeley National Laboratory under Contract DE-AC02-05CH11231. COGENT code development is supported as part of the US DOE Edge Simulation Laboratory Collaboration.

### References

- [1] BURRELL, K. H., “Effects of  $E \times B$  velocity shear and magnetic shear on turbulence and transport in magnetic confinement devices”, *Phys. Plasmas* **4** (1997) 1499.
- [2] KAGAN, G., CATTO, P., “Neoclassical ion heat flux and poloidal flow in a tokamak pedestal”, *Plasma Phys. Control. Fusion* **52** (2010) 055004.
- [3] PUSZTAI, I., CATTO, P., “Neoclassical plateau regime transport in a tokamak pedestal”, *Plasma Phys. Control. Fusion*, **52** (2010) 075016.
- [4] HELANDER, P., SIGMAR, D. J., *Collisional Transport in Magnetized Plasmas*, Cambridge University Press (2002).
- [5] KAGAN, G., et al., “The effect of the radial electric field on neoclassical flows in a tokamak pedestal”, *Plasma Phys. Control. Fusion*, **53** (2011) 025008.
- [6] DORF, M. A., et al., “Progress with the COGENT Edge Kinetic Code: Collision Operator Options”, *Contr. Plasma Phys.* **52** (2012) 518.
- [7] DORF, M. A., et al., “Simulation of Neoclassical Transport with the Continuum Gyrokinetic Code COGENT”, *Phys. Plasmas* (submitted for publication).
- [8] DORR, M. R., et al., “Numerical Simulation of Phase Space Advection in Gyrokinetic Models of Fusion Plasmas” (Proc. SciDAC 2010 Conf. Tennessee, 2010).
- [9] WINSOR, N., et al., “Geodesic Acoustic Waves in Hydromagnetic Systems”, *Phys. Fluids* **11** (1968) 2448.
- [10] GAO, Z., et al., “Eigenmode analysis of geodesic acoustic modes” *Phys. Plasmas* **15** (2008) 072511.
- [11] ABEL, I. G., “Linearized model Fokker–Planck collision operators for gyrokinetic simulations. I. Theory”, *Phys. Plasmas* **15** (2008) 122509.
- [12] PARRA, F. I., CATTO, P. J., “Limitations of gyrokinetics on transport time scales”, *Plasma Phys. Control. Fusion* **50** (2008) 065014.
- [13] HIRSHMAN, S. P., “The ambipolarity paradox in toroidal diffusion, revisited”, *Nucl. Fusion* **18** (1978) 917.
- [14] CHANG, C. S., HINTON, F. L., “Effect of finite aspect ratio on the neoclassical ion thermal conductivity in the banana regime”, *Phys. Fluids* **25** (1982) 1493.
- [15] HOULBERG, W. A., et al., “Bootstrap current and neoclassical transport in tokamaks of arbitrary collisionality and aspect ratio”, *Phys. Plasmas* **4** (1997) 3230.
- [16] KAGAN, G., CATTO, P., “Arbitrary poloidal gyroradius effects in tokamak pedestals and transport barriers”, *Plasma Phys. Control. Fusion* **50** (2008) 085010.